# Lowering of the Interstitial Fluid Pressure as a Result of Tissue Compliance Changes during High Intensity Focused Ultrasound Exposure: Insights from a Numerical Model

E. Sassaroli*, B. E. O'Neill**
The Methodist Hospital Research Institute, Houston, TX, 77030, USA
*elisabettasassaroli@gmail.com, **beoneill@tmhs.org

**Abstract:** Interstitial fluid pressure (IFP) is elevated in tumors. This may constitute a significant physiological barrier to drug delivery to solid tumors. Owing to this elevated IFP, the interstitial fluid velocity (IFV) is negligible throughout the tumor but significant near the tumor margin. Any therapeutic strategy that can lower the IFP will likely improve drug convection within the tumor and decrease convection of drugs from the tumor margin. High intensity focused ultrasound (HIFU) operated in thermal mode has been shown to reduce the IFP and to improve the penetration of therapeutics in tumors. We have used a mathematical model to simulate the effect of HIFU on the IFP and IFV. We have shown that a reduction of the IFP as a result of HIFU exposure facilitates fluid convection and macromolecule distribution within the exposed area and reduces fluid convection and macromolecule wash out at its margin.

**Keywords:** High Intensity Focused Ultrasound, Targeted Drug Delivery, Soft Tissue, Linear Biphasic Models.

## 1. Introduction

The ability of HIFU to concentrate the acoustic energy on a focal spot, measuring a few millimeters in diameter in organs at depth within the body without damaging the overlying and surrounding tissue has been investigated for several years largely for applications to thermal ablation (destruction) of tumor tissue [1]. An emerging application of HIFU is targeted drug delivery to tumors. Efficient delivery of therapeutic agents into solid tumors still remains a big challenge in medicine [2].

Owing to the abnormal structure and function of blood and lymphatic vessels in tumors, the IFP is elevated in tumors [2]. Since elevated IFP may constitute a major physiological barrier to drug delivery in solid tumors, novel strategies are needed to overcome this barrier. HIFU has been reported to increase the uptake of therapeutics in a number of tumor models in experimental studies [3-5] and to reduce IFP [5].

In order to gain some insight into the effect of HIFU on the transport of fluid and macromolecules in tumor tissue, we present here a mathematical model. This model consists of a macroscopic fluid transport model able to predict the pressure and the velocity distributions. This model is applied to tumor tissue in a simplified case of a homogeneous, alymphatic spherical tumor.

## 2. Materials and Methods

### 2.1 Description of Model

A tissue can be divided into three compartments: cellular, vascular, and interstitial. As compared to normal tissue however tumor tissue is more spatially heterogeneous with large differences in the vasculature and in the cells between different regions. In our model, these differences have been averaged out as discussed by Baxter and Jain [6] who proposed and validated a mathematical model for tumor tissue in which the microscopic features such as blood vessels, cells and interstitial space are not considered explicitly. Their goal was to determine the steady-state IFP and IFV profiles over a length scale on the order of the tumor radius and they were able to successfully predict that the IFP is elevated in tumors.

The interstitium or interstitial space is a connective tissue giving support and protection to the blood vessels and cells of a given organ. It is primarily composed of an hydrated gel of negatively charged macromolecules: the glycosaminoglycan chains (GAGs) (long polymer of amino sugars) in a framework of fibrous proteins and connective tissue cells [7]. Collagen is the most abundant fibrous protein of the interstitium and forms a network of collagen fibers. The characteristic cell type of the interstitial connective tissue is the fibroblast.

In order to incorporate the effect of tissue compliance changes as a result of HIFU exposure, we have made use of an extension of the Baxter and Jain model proposed by Netti *et al.* [8]. Netti's model includes the interstitium matrix mechanics (solid stress and deformation) into the Baxter and Jain model and reduces to it at steady state.

In this study, we adopt Netti's model to describe the time dependent changes of the IFP and IFV as result of HIFU exposure. The idea is to model the preliminary stage of inflammation caused by HIFU exposure which is characterized by a rapid fluid accumulation (edema) in the interstitium. Edema formation is initially caused by a transient lowering of the IFP that then increases as the fluid accumulates in the interstitium.

The interstitium has a natural tendency to swell owing to the presence of GAGs macromolecules. At equilibrium, the swelling pressure of the GAGs is counteracted by the collagen fibrils-fibroblast system [7,9]. During FUS exposure, the collagen fibrils-fibroblast system is damaged and cannot balance the swelling pressure of the GAGs that now can swell by accumulating a lot of fluid in a rapid way for several minutes. From a phenomenological point of view, we can assume that in the region affected by HIFU, the aggregate modus of the interstitium (inverse of the compliance) is suddenly affected. A temporary increase of H or decrease of the compliance, reduces the interstitium fluid pressure (IFP) with the result that more fluid will extravasate into the interstitium.

### 2.2 Governing Equations

Netti's model for tumor tissue is based on the linear biphasic model of soft tissue developed by Mow *et al.* [10]. Mow's model assumes that the interstitium is composed of two phases: an interstitial fluid phase and an elastic solid phase which are intrinsically incompressible and undergo only small deformations. The solid matrix phase consists of a porous-permeable, elastic-solid matrix. The tissue as a whole is compressible through exudation of fluid. It is further assumed that the solid phase is isotropic and linearly elastic.

Since the intercapillary distance (100 μm) is two orders of magnitude smaller than the macroscopic dimension of a tumor (1 cm), the capillary network can be modeled as a continuous distribution instead of discrete fluid source/sink channels. As a consequence, the Mow's equations of soft tissue can be combined to obtain [8,10]

$$\nabla \cdot \left[\phi \boldsymbol{v} + (1-\phi)\frac{\partial \boldsymbol{u}}{\partial t}\right] = \Omega(\boldsymbol{r}, t) \qquad (1)$$

where $\phi$ is the volume fluid fraction, $\boldsymbol{v}$ is the IFV, $\boldsymbol{u}$ is the tissue displacement and $\Omega(\boldsymbol{r}, t)$ is the fluid source term ($s^{-1}$) given by the Starling equation:

$$\Omega(\boldsymbol{r}, t) = \frac{J_v S}{V} = \frac{L_p S}{V}(P_e - P_i) \qquad (2)$$

where $J_v$ the fluid flux across the vascular wall, $L_p$ is the average hydraulic conductivity coefficient of the capillary; *S/V* is the surface area of vessel wall per unit volume of tissue; $P_e$ is the effective vascular pressure $P_e = P_v - \sigma(\pi_V - \pi_i)$. The difference between the average vascular pressure $P_v$ and average IFP $P_i$ is countered by the effective oncotic pressure ($\sigma(\pi_c - \pi_i)$). The parameters $\sigma$, $\pi_V$ and $\pi_i$ are, respectively, the average osmotic reflection coefficient of plasma proteins, the colloid osmotic pressure of plasma, and the colloid osmotic pressure of interstitial fluid. This model assumes that there is no functional lymphatic vasculature inside the tumor to drain interstitial fluid.

The relative movement between the fluid and solid phases is described by the generalized form of Darcy's law:

$$\phi\left[\boldsymbol{v} - \frac{\partial \boldsymbol{u}}{\partial t}\right] = -K\nabla P_i \qquad (3)$$

where $K$ is the average tissue hydraulic conductivity.

The momentum balance for the tissue under the hypothesis of negligible inertial and body forces is

$$\nabla \cdot T = 0 \qquad (4)$$

where $T$ represents the effective tissue stress tensor. Assuming the solid matrix to behave as a linear elastic material in the limit of small strain, the constitutive equation for the tissue is

$$T = -P_i I + \tau \qquad (5)$$

where $\tau = \lambda e I + 2\mu\epsilon$ is the solid matrix stress tensor with $\lambda$ and $\mu$ are the Lame' constants, $I$ is the unity tensor, $e$ is the tissue dilatation and $\epsilon$ is the strain tensor $\epsilon = \frac{1}{2}[\nabla \boldsymbol{u} + \nabla \boldsymbol{u}^T]$.

Eq. 3 implies that the relative velocity field (i.e. $\boldsymbol{v} - \frac{\partial \boldsymbol{u}}{\partial t}$) is irrotational. Furthermore, from the hypothesis of elasticity of the solid phase and assuming axial symmetry, it follows that the solid displacement and the fluid velocity fields are both irrotational. These assumptions allow to combine the above equations (1-5) to obtain the following PDE for the dilatation $e$

$$\frac{\partial e}{\partial t} - KH\nabla^2 e + H\frac{L_p S}{V} e = \frac{L_p S}{V} P_e \qquad (6)$$

where $H = 2\mu + \lambda$ is the aggregate modulus which is the inverse of the compliance. As a consequence of HIFU exposure, we assume that the tissue in the focal region experiences a sudden change in the interstitium aggregate modulus H from $H_0 = 2\mu_0 + \lambda_0$ to a value $H = 2\mu + \lambda$ and therefore we solve Eq. (6) assuming $H$ to be time dependent. In tumors, $\pi_V \approx \pi_i$ and therefore $P_e$ is approximately the same as $P_v$.

The determination of the dilation $e$, allows to determine the IFP through $\nabla \mathrm{e} = \frac{\nabla \mathrm{P_i}}{2\mu+\lambda}$, the tissue displacement **u** thorough $e = \nabla \cdot \boldsymbol{u}$, and the fluid velocity $\boldsymbol{v}$ through Eq. (3).

### 2.3 Use of Comsol Multiphysics

Eq. (6) has been solved numerically using Comsol Multiphysics 4.3 as a 2D axisymmetric model. Denoting with $R$ the tumor radius and introducing the dimensionless cylindrical coordinates $\hat{r} = \frac{r}{R}$, $\hat{z} = \frac{z}{R}$, the dimensionless time $\hat{t} = \frac{t}{t_0}$ with $t_0 = R^2/(KH_0)$ and the time dependent ratio $X = \frac{H}{H_0}$ where $H_0$ is the steady-state aggregate modulus, Eq. (6) reads

$$\frac{1}{X}\frac{\partial \hat{e}}{\partial \hat{t}} - \nabla^2 \hat{e} + \alpha^2 \hat{e} = \frac{\alpha^2}{X} \qquad (7)$$

with $\alpha = R\sqrt{\frac{L_p S}{KV}}$. The steady-state dilation $e_0$ is given by $e_0 = \frac{P_v}{H_0}$ and $\hat{e} = e/e_0$.

The model geometry consists of three sub-domains: an ellipsoid shape region of dimensionless radius $a/R$ ($a$ semi-minor axis) and axial length $l/R$ ($l$ semi-major axis) consisting of tumor tissue exposed to HIFU, surrounded by tumor tissue of radius one. The tumor is surrounded by normal tissue of radius $R_N$.

Eq. (7) have been solved using the Heat Transfer Module. In the ellipsoidal domain, the ratio $X$ is assumed to vary as a step function. A step function can be readily implemented with Comsol Multiphysics 4.3. In the surrounding tumor tissue, Eq. (9) is solved with $X = 1$.

In normal tissue, the pressure in the left-hand side of Eq. (6) can be identified as the pressure at which the efflux from the vasculature equals influx into the lymphatics keeping an average constant IFP which in most soft tissues is close to zero. Therefore, we can assume the left-hand side of Eq. (6) to be zero and solve Eq. (7) with the left-hand side equal to zero and the parameter $\alpha$ having a different value in normal tissue as compared to the one in tumor tissue.

The initial condition for this model can be obtained from the steady-state analytical solutions of the Netti's model or equivalently of the Baxter and Jain model, or simply by solving the model at steady-state. The agreement between the Comsol finite element solutions and the analytical solutions is excellent.

For the boundary conditions, we assume the no-flux boundary condition (axial symmetry) at $\hat{r} = 0$ and at large distance we assume normal tissue conditions i.e. at $\hat{r} = R_N$, $\hat{e} = 0$ using the Comsol open boundary condition feature.

The determination of $\hat{e}$ allows to determine all the other quantities defined in Sec. 2.2 by making use of the General Equation Module and the post-processing capability of Comsol.

## 3. Results

### 3.1 Interstitial Fluid Pressure

In solving the model equations, we have assumed the tumor radius $R = 0.4\ cm$, the parameters $\alpha = 10$, $\alpha_N = 1.39$. These values are within the range of values provided in [11].

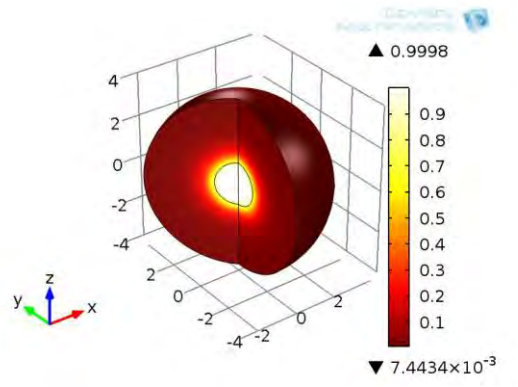


**Figure 1**. Relative IFP distribution in a spherical tumor surrounded by normal tissue.

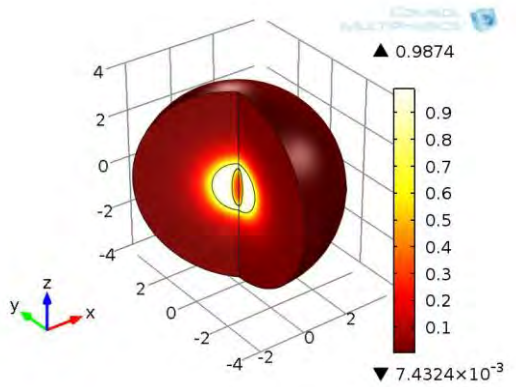


**Figure 2**. Relative IFP drop in a spherical tumor surrounded by normal tissue at the HIFU affected volume.

Fig. 1 shows the relative IFP for $\hat{t} = 0$. The relative IFP is defined as the IFP divided by the average macrovascular pressure. This is the IFP of the Baxter and Jain model which predicts a relatively uniform IFP throughout the tumor decreasing precipitously in the tumor margin. If the relative aggregate modulus of the interstitium $X(\hat{t})$ is assumed to increase by a factor of 10 in a time $\delta\hat{t} = 0.7$ as a result of HIFU exposure, then the model predicts a lowering of the IFP in the focal region as may be seen in Fig. 2 where the relative IFP has been plotted for the time $\hat{t} = 1$.

### 3.2 Interstitial Fluid Velocity

Unlike IFP, there are no reported measurements of IFV profiles in tumors. In cases in which experimental data are difficult to obtain, a mathematical model can provide useful insight. The components $(\hat{v}_r, \hat{v}_z)$ of the IFV for a tumor tissue surrounded by normal tissue have been plotted as 1D plots in Figs. 3 and 4 for two particular directions respectively the axial direction and the radial direction at different times. In these plots, for the purpose of illustration we have assumed the volume fluid fraction $\phi$ to be constant and the same for normal and tumor tissue and equal to 0.3. Plots similar to Fig. 3 and 4 can be obtained in all the other directions. The components $\hat{v}_z$ and $\hat{v}_r$ have been normalized with respect to the velocity at the outer edge of the tumor at $\hat{t} = 0$ which is the same in magnitude for both components. The result at $\hat{t} = 0$ reproduces the one of the Baxter and Jain model predicting the fluid convection to be negligible throughout the tumor but significant near the tumor margin and directed away from the tumor. For the change of the relative aggregate modulus of the interstitium as given in Fig. 2, the plots also indicate that the lowering of the IFP facilitates fluid convection inside the HIFU affected volume, significant decrease fluid loss at the HIFU exposure boundary with the velocity directed towards the tumor center and somewhat reduces fluid loss at the tumor boundary.

Thus, therapeutic agents injected before the lowering of the IFP might be washed out directly from peripheral vessels across the tumor boundary, but delivery of injected therapeutics after the lowering of the IFP would be improved

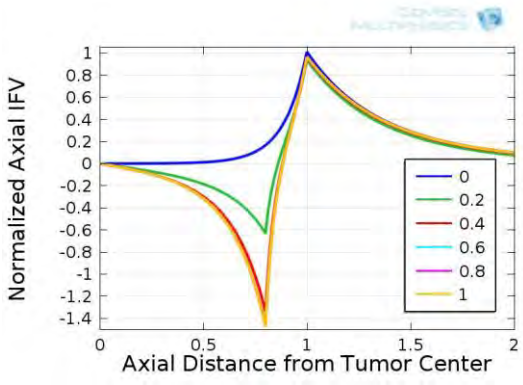


**Figure 3**. Normalized IFV along the axial direction as a function of distance from the tumor center at different times. Relative distance <1 represents region within the tumor, whereas >1 represents region outside of the tumor.

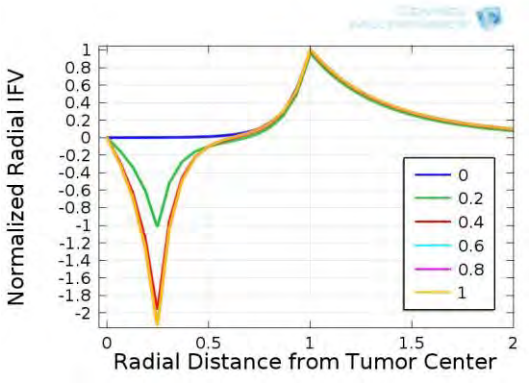


**Figure 4**. Normalized IFV along the radial direction as a function of distance from the tumor center at different times. Relative distance <1 represents region within the tumor, whereas >1 represents region outside of the tumor.

inside the tumor, whereas less drugs will be washed out of the HIFU exposure margin.

## 4. Conclusions

It is well established that IFP is elevated in tumors and this phenomenon may influence the efficient delivery of therapeutic agents in tumors If one assumes that the delivery of anti-tumor agents is dependent at least in part on the pressure gradient for filtration into a tumor, a way to enhance tumor uptake is to reduce the IFP. Our simulations seem to confirm this fact since a lowering of the IFP appears to increase intra-tumor fluid convection and facilitates distribution and penetration of macromolecules throughout the tumor primarily at the HIFU affected regions. Furthermore it appears to decrease fluid loss at the HIFU boundary and to a much less extent at the tumor boundary, therefore decreasing the loss of fluid and therapeutics into the surrounding tissue.

## 5. References

1. Ter Haar GR, Therapeutic applications of ultrasound, *Prog Biophys Mol Biol*, **93**, 111-29 (2007)
2. Jain RK, Barriers to drug delivery in solid tumors, *Sci Am*, **271**, 58–65 (1994)
3. Dittmar KM, Xie J, Hunter F, Trimble C, Bur M, Frenkel V and Li KC, Pulsed high-intensity focused ultrasound enhances systemic administration of naked DNA in squamous cell carcinoma model: Initial experience, *Radiology*, **235**, 541–6 (2005)
4. Chen X, Cvetkovic D, Ma CM and Chen L, Quantitative study of focused ultrasound enhanced doxorubicin delivery to prostate tumor in vivo with MRI guidance, *Med Phys*, **39**, 2780-6 (2012)
5. Watson KD, Lai CY, Qin S, Kruse DE, Lin YC, Seo JW, Cardiff RD, Mahakian LM, Beegle J, Ingham ES, Reed RK and Ferrara KW, Ultrasound increases nanoparticle delivery by reducing intratumoral pressure and increasing transport in epithelial and epithelial-mesenchymal transition tumors, *Cancer Res*, **72**, 1485-93 (2012)
6. Baxter LT and Jain RK, Transport of fluid and macromolecules in tumors. I. Role of interstitial pressure and convection, *Microvasc Res*, **37**, 77–104 (1989)
7. Aukland K and Reed RK, Interstitial-lymphatic mechanisms in the control of extracellular fluid volume, *Physiol Rev*, **73**,1-78 (1993)
8. Netti PA, Baxter LT, Boucher Y, Skalak R and Jain RK, Time-dependent behavior of interstitial fluid pressure in solid tumors: implications for drug delivery, *Cancer Res*, **55**, 5451–8 (1995)
9. Wiig H, Rubin K and Reed RK, New and active role of the interstitium in control of interstitial fluid pressure: potential therapeutic consequences, *Acta Anaesthesiol Scand*, **47**, 111-21 (2003)
10. Mow VC, Kuei SC, Lai WM and Armstrong CG, Biphasic creep and stress relaxation of articular cartilage in compression: theory and experiments, *J Biomech Eng*, **102**, 73-84 (1980)
11. Jain RK, Tong RT, and Munn LL, Effect of Vascular Normalization by Antiangiogenic Therapy on Interstitial Hypertension, Peritumor Edema, and Lymphatic Metastasis: Insights from a Mathematical Model, *Cancer Res*, **67**, 2729–35 (2007)

## 6. Acknowledgements

The authors gratefully acknowledge Dr. King Li and NIBIB (R01-EB009009) for supporting this work.